

Synthesis, Crystal Structure, and Magnetic Properties of Tetraphenylarsonium Tetrachloro(oxalato)rhenate(IV) and Bis(2,2'-bipyridine)tetrachloro(μ -oxalato)copper(II)rhenium(IV)

Raúl Chiozzone,^{1a} Ricardo González,^{1a} Carlos Kremer,^{*,1a} Giovanni De Munno,^{1b} Joan Cano,^{1c} Francesc Lloret,^{1c} Miguel Julve,^{1c} and Juan Faus^{*,1c}

Cátedra de Química Inorgánica, Facultad de Química de la Universidad de la República, Montevideo, Uruguay, Dipartimento di Chimica, Università degli Studi della Calabria, 87030 Arcavacata di Rende, Cosenza, Italy, and Departamento de Química Inorgánica, Facultad de Química de la Universidad de Valencia, Dr. Moliner 50, 46100 Burjassot, Valencia, Spain

Received April 6, 1999

Two new rhenium(IV) compounds of formula $(\text{AsPh}_4)_2[\text{ReCl}_4(\text{ox})]$ (**1**) and $[\text{ReCl}_4(\mu\text{-ox})\text{Cu}(\text{bipy})_2]$ (**2**) ($\text{AsPh}_4 =$ tetraphenylarsonium cation, $\text{ox} =$ oxalate anion, and $\text{bipy} =$ 2,2'-bipyridine) have been synthesized and their crystal structures determined by single-crystal X-ray diffraction. **1** and **2** crystallize in the monoclinic system, space groups $P2_1/c$ and $P2_1/n$, respectively, with $a = 22.250(5)$ Å, $b = 11.245(3)$ Å, $c = 19.089(4)$ Å, $\beta = 96.59(2)^\circ$, and $Z = 4$ for **1** and $a = 9.421(2)$ Å, $b = 16.909(4)$ Å, $c = 16.179(4)$ Å, $\beta = 93.97(2)^\circ$, and $Z = 4$ for **2**. The structure of **1** is made up of $[\text{ReCl}_4(\text{ox})]^{2-}$ anions and AsPh_4^+ cations held united by electrostatic forces. Rhenium(IV) is hexacoordinate, with two oxygens of a chelating ox and four chlorine atoms building a distorted octahedron around the metal atom. There is no contact between the $[\text{ReCl}_4(\text{ox})]^{2-}$ anions, the shortest $\text{Re}\cdots\text{Re}$ and $\text{Cl}\cdots\text{Cl}$ distances being 10.345 and 7.209 Å, respectively. This anionic complex is coordinated to a $[\text{Cu}(\text{bipy})_2]^{2+}$ cation in **2**, through one oxalate–oxygen, giving a neutral heterometallic dinuclear unit. The Cu(II) ion shows a very distorted five-coordinated geometry, four bipy-nitrogens occupying the equatorial positions and the oxygen atom the apical one. The basal plane geometry is distorted toward the tetrahedron, the dihedral angle between the mean planes of the two bipy ligands is $37.6(2)^\circ$. These $[\text{ReCl}_4(\mu\text{-ox})\text{Cu}(\text{bipy})_2]$ units are arranged in such a way that a chlorine atom of one of them points toward the copper atom of the neighboring one, forming helicoid chains. The intrachain $\text{Re}\cdots\text{Cu}$ distances through chloro and oxalato bridges are 4.658 and 4.798 Å, respectively. The magnetic behavior of **1** and **2** has been investigated over the temperature range 1.8–300 K. **1** is a magnetically diluted Re(IV) complex, the great value of zero-field splitting of the ground level ($D = 60$ cm^{-1}) accounting for the variation of χ_{MT} with T in the low-temperature range. **2** behaves as a ferrimagnetic chain, with weak antiferromagnetic interactions between Re(IV) and Cu(II) through oxalato and single chloro bridges.

Introduction

There is currently a great interest in the magnetic properties of polynuclear complexes of transition metals. Many compounds, ranging from simple dinuclear species to coordination polymers with tridimensional lattices, have been characterized in the last twenty years. However, up to now the study of the interaction between magnetic centers has been generally restricted to metal ions belonging to the first transition series. Heavier elements have been largely ignored in this respect, and so no mention is made of metal ions of the second and third transition series in a recent and excellent book on molecular magnetism.²

The larger splitting of d orbitals and the smaller interelectronic repulsion which occur in the complexes with the heavy transition metal ions account for the low-spin configuration that they exhibit. This means that ions with an even number of d electrons are very often diamagnetic. Even though they have unpaired electrons, the large splitting of the ground term produced by

the high value of the spin–orbit coupling constant may stabilize a nonmagnetic level.^{3,4} Moreover, polynuclear species are frequently diamagnetic clusters because of the greater tendency to form metal–metal bonds. These features explain the low interest in the magnetic properties of 4d and 5d metal ions.

This situation could be changing already. As indicated recently by Kahn *and* et al.,⁵ once the magnetic interaction between 3d metal ions is reasonably well understood, the study of systems involving 4d or 5d metal ions becomes very interesting. The greater orbital diffuseness and spin–orbit coupling may affect the nature and magnitude of the interaction between magnetic centers.

We are interested in the synthesis, structural characterization and magnetic properties of polynuclear complexes containing Re(IV) and first-row transition metal ions. Rhenium(IV), a $5d^3$ ion, seems to us a good choice because it forms usually octahedral complexes which are reasonably stable against redox

(3) Cotton, F. A.; Wilkinson, G. *Advanced Inorganic Chemistry*, 5th ed.; Wiley-Interscience: New York, 1988; p 777.

(4) Boudreaux, E. A.; Mulay L. N. *Theory and Applications of Molecular Paramagnetism*; Wiley-Interscience: New York, 1976.

(5) Larionova, J.; Mombelli, B.; Sanchiz, J.; Kahn, O. *Inorg. Chem.* **1998**, *37*, 679.

(1) (a) Universidad de la República, Montevideo. (b) Università degli Studi della Calabria. (c) Universidad de Valencia.

(2) Kahn, O. *Molecular Magnetism*; VCH: New York, 1993.

processes and inert to ligand substitution.⁶ Moreover, the ground electronic state is a $4A_{2g}$ term with three unpaired electrons. The absence of orbital angular moment keeps off any complication due to the high value of the spin-orbit coupling constant (λ ca. 1000 cm^{-1} in the free ion). Spin-orbit coupling is only manifested in the $g < 2$ value of the only occupied level (second-order effects) within the context of the Russell-Saunders approach. However, because of the large values of the ligand field splitting and the small value of the bielectronic repulsion, an intermediate coupling scheme would be more convenient. The magnetic properties of mononuclear hexahalo complexes, $[\text{ReX}_6]^{2-}$, have been studied with some detail⁷⁻⁹ and these studies revealed the occurrence of an intermolecular antiferromagnetic interaction whose magnitude depends on the nature of the halogen atom and the halogen-halogen separation between ions in the solid. The magnetic exchange is relatively strong in the potassium salts and very weak when using bulky organic cations.

Our approach involves the synthesis of mononuclear Re(IV) complexes which can act as ligands toward first-row transition metal ions. The well-known bis(didentate) character of the oxalato group and its remarkable ability to mediate magnetic interactions between the metal centers which are bridged by it¹⁰ led us to prepare a mono-oxalato rhenate(IV) complex.

In the past, a significant amount of work has been devoted to the synthesis of oxalato-containing Re(IV) complexes.¹¹ However, the reported experimental procedures are not entirely reproducible, and they yield a mixture of several products not well characterized. An important step in this work was the determination of the crystal structure of the dimer compound $\text{K}_4[(\text{ox})_2\text{Re}(\mu\text{-O})_2\text{Re}(\text{ox})_2]\cdot 3\text{H}_2\text{O}$.¹² Its diamagnetism is consistent with the occurrence of a multiple metal-metal bond. As far as we know, no paramagnetic oxalato-containing Re(IV) complex has been described up to now.

In this work, we report the synthesis, crystal structure, and magnetic properties of two new Re(IV) compounds of formula $(\text{AsPh}_4)_2[\text{ReCl}_4(\text{ox})]$ (**1**) and $[\text{ReCl}_4(\mu\text{-ox})\text{Cu}(\text{bipy})_2]$ (**2**) (AsPh_4 = tetraphenylarsonium cation, ox = oxalato anion, and bipy = 2,2'-bipyridine). **1** is a paramagnetic, oxalato-Re(IV) mononuclear complex, and **2** is an oxalato-bridged heterodinuclear Re(IV)-Cu(II) complex.

Experimental Section

Materials. Ammonium perrhenate(VII), copper(II) trifluoromethanesulfonate, tetrabutylammonium bromide, tetraphenylarsonium chloride monohydrate, oxalic acid dihydrate, and 2,2'-bipyridine were purchased from commercial sources and used as received. $\text{K}_2[\text{ReCl}_6]$ was prepared following a literature procedure.¹³ This compound was transformed into the tetrabutylammonium salt, $(\text{NBu}_4)_2[\text{ReCl}_6]$, by metathetic reaction in hot 0.5 mol L^{-1} hydrochloric acid.

Synthesis of the Complexes. $(\text{AsPh}_4)_2[\text{ReCl}_4(\text{ox})]$ (1**).** A mixture of 300 mg of $(\text{NBu}_4)_2[\text{ReCl}_6]$ (0.34 mmol) and 260 mg of oxalic acid dihydrate (2.0 mmol) was heated under reflux in 15 mL of 2-propanol. Then, 280 μL of triethylamine (2.0 mmol) was added slowly. The heating was stopped 15 min after the complete dissolution of the reagents, and the solution was allowed to cool at room temperature. The light green precipitate, mainly $(\text{HNEt}_3)_2[\text{ReCl}_4(\text{ox})]$, was filtered promptly and washed with 2-propanol ($2 \times 2\text{ mL}$) and diethyl ether ($2 \times 2\text{ mL}$). The solid was dissolved in 15 mL of hot ethanol, and a solution of 325 mg of $\text{AsPh}_4\text{Cl}\cdot\text{H}_2\text{O}$ (0.77 mmol) in the minimum amount of hot ethanol was added. Bright light green plates of the final product are obtained by slow evaporation of the solvent at room temperature. The crystals were washed with cold ethanol ($3 \times 1\text{ mL}$) and diethyl ether. Yield: 45–55%. Suitable crystals for X-ray diffraction studies were obtained by slow evaporation from a 1:1 ethanol-acetonitrile mixture. Anal. Calcd for $\text{C}_{50}\text{H}_{40}\text{As}_2\text{Cl}_4\text{O}_4\text{Re}$ (**1**): C, 50.78; H, 3.41%. Found: C, 50.90; H, 3.38. IR: bands associated to the oxalato ligand appear at (cm^{-1}) 1712 (vs), 1680 (w), 1666 (w), 1338 (s), and 799 (s).

$(\text{NBu}_4)_2[\text{ReCl}_4(\text{ox})]$. This compound was obtained following the same procedure described above until the precipitation of $(\text{HNEt}_3)_2[\text{ReCl}_4(\text{ox})]$. This solid, if not filtered, redissolved nearly completely in the solution on standing a few days. The solution was left to evaporate near to dryness, and the green crystals were washed with water ($2 \times 2\text{ mL}$), cold 2-propanol ($2 \times 1\text{ mL}$), and diethyl ether ($2 \times 2\text{ mL}$). Yield: 50–60%. Anal. Calcd for $\text{C}_{34}\text{H}_{72}\text{N}_2\text{Cl}_4\text{O}_4\text{Re}$: C, 45.33; H, 8.06; N, 3.11. Found: C, 44.99; H, 7.49; N, 3.06. IR: bands associated to the oxalato ligand appear at (cm^{-1}) 1713 (vs), 1694 (sh), 1664 (m), 1336 (s), and 801 (s).

$[\text{ReCl}_4(\mu\text{-ox})\text{Cu}(\text{bipy})_2]$ (2**).** A solution 45 mg of $(\text{NBu}_4)_2[\text{ReCl}_4(\text{ox})]$ (0.05 mmol) in 25 mL of acetonitrile was added to a solution of 18 mg of copper(II) trifluoromethanesulfonate (0.05 mmol) and 15.6 mg of 2,2'-bipyridine (0.10 mmol) in 25 mL of acetonitrile. Dark green scales of **2** appeared in some minutes, and crystallization was complete after some days. The solid was filtered and washed with acetonitrile ($2 \times 2\text{ mL}$). Yield: over 85%. Polyhedral dark green single crystals suitable for X-ray diffraction studies were obtained by the same procedure but reducing the amount of 2,2'-bipyridine to a half. Anal. Calcd for $\text{C}_{22}\text{H}_{16}\text{N}_4\text{Cl}_4\text{O}_4\text{CuRe}$ (**2**): C, 33.37; H, 2.04; N, 7.07. Found: C, 34.23; H, 1.90; N, 7.15. IR: bands associated to the oxalato ligand appear at (cm^{-1}) 1710 (vs), 1678 (m), 1358 (s), and 802 (s).

Physical Techniques. The IR spectra (KBr pellets) was recorded with a Perkin-Elmer 1750 FTIR spectrometer. Magnetic susceptibility measurements (2.0–300 K) were carried out with a Quantum Design SQUID magnetometer under an applied magnetic field of 1 T at high temperature and only 50 G at low temperature to avoid any problem of magnetic saturation. The device was calibrated with $(\text{NH}_4)_2\text{Mn}(\text{SO}_4)_2\cdot 6\text{H}_2\text{O}$. The corrections for the diamagnetism were estimated from Pascal constants.

X-ray Data Collection and Structure Refinement. Crystals of dimensions $0.40 \times 0.38 \times 0.25$ (**1**) and $0.40 \times 0.32 \times 0.36\text{ mm}$ (**2**) were mounted on a Siemens R3m/V automatic four-circle diffractometer and used for data collection. Diffraction data were collected at room temperature by using graphite monochromated $\text{Mo K}\alpha$ radiation ($\lambda = 0.71073\text{ \AA}$) with the ω (**1**) and $\omega-2\theta$ (**2**) scan methods. The unit cell parameters were determined from least-squares refinement of the setting angles of 25 reflections in the 2θ range of $15\text{--}30^\circ$. Information concerning crystallographic data collection and structure refinement is summarized in Table 1. Examination of two standard reflections, monitored after 98 reflections, showed no sign of crystal deterioration. Lorentz-polarization and absorption corrections were applied to the intensity data. The maximum and minimum transmission factors were 0.184 and 0.161 for **1** and 0.184 and 0.118 for **2**. Of the 7506 (**1**) and 6019 (**2**) measured reflections in the 2θ range $3\text{--}54^\circ$ with index ranges $-22 \leq h \leq 26$, $0 \leq k \leq 13$, and $0 \leq l \leq 22$ (**1**) and $-12 < h < 12$, $0 \leq k \leq 21$, and $0 \leq l \leq 20$ (**2**), 6732 (**1**) and 5430 (**2**) were unique. From these, 5317 (**1**) and 4523 (**2**) were observed [$I > 3\sigma(I)$] and used for the refinement of the structures.

The structures were solved by standard Patterson methods and subsequently completed by Fourier recycling. All non-hydrogen atoms were refined anisotropically. The hydrogen atoms were set in calculated

- (6) (a) Rouschias, G. *Chem. Rev.* **1974**, *74*, 531. (b) Conner, K. A.; Walton, R. A. In *Comprehensive Coordination Chemistry*; Wilkinson, G., Gillard, R. D., McCleverty, J. A., Eds.; Pergamon Press: New York, 1987; Vol. 4, p 165.
- (7) Figgis, B. N.; Lewis, J.; Mabbs, F. E. *J. Chem. Soc.* **1961**, 3138.
- (8) Spitsyn, V. I.; Zhiron, A. I.; Subbotin, M. Yu.; Kazin, P. E. *Russ. J. Inorg. Chem.* **1980**, *25*, 556.
- (9) (a) Mrozinski, J. *J. Bull. Ac. Pol. Chim.* **1978**, *26*, 789. (b) Mrozinski, J. *J. Bull. Ac. Pol. Chim.* **1980**, *28*, 559. (c) Malecka, J.; Jager, L.; Wagner, Ch.; Mrozinski, J. *Pol. J. Chem.* **1998**, *72*, 1879.
- (10) Muñoz, M. C.; Julve, M.; Lloret, F.; Faus, J.; Andruh, M. *J. Chem. Soc., Dalton Trans.* **1998**, 3125 and refs 1–11 therein.
- (11) Atkinson, J. W.; Hong, M.; House, D. A.; Kyrtis, P.; Li, Y.; Nasreldin, M.; Sykes, A. G. *J. Chem. Soc., Dalton Trans.* **1995**, 3317 and references therein.
- (12) Lis, T. *Acta Crystallogr., Sect. B* **1975**, *31*, 1594.
- (13) Kleinberg, J., Ed. *Inorganic Syntheses*; McGraw-Hill: New York, 1963; Vol. VII, p 189.

Table 1. Summary of Crystal Data^a for [As(C₆H₅)₄]₂[ReCl₄(ox)] (**1**) and [ReCl₄(μ-ox)Cu(bipy)]₂ (**2**)

	1	2
empirical formula	C ₅₀ H ₄₀ As ₂ Cl ₄ O ₄ Re	C ₂₂ H ₁₆ Cl ₄ CuN ₄ O ₄ Re
<i>M</i>	1182.7	791.9
crystal system	monoclinic	monoclinic
space group	<i>P</i> 2 ₁ / <i>c</i>	<i>P</i> 2 ₁ / <i>n</i>
<i>a</i> , Å	22.250(5)	9.421(2)
<i>b</i> , Å	11.245(3)	16.909(4)
<i>c</i> , Å	19.089(4)	16.179(4)
β, deg	96.59(2)	93.97(2)
<i>V</i> , Å ³	4745(2)	2571.1(10)
<i>Z</i>	4	4
<i>D</i> _c /Kg m ⁻³	1.656	2.046
<i>F</i> (000)	2324	1520
μ(Mo Kα), cm ⁻¹	42.14	59.84
<i>R</i> ^b	0.034	0.044
<i>R</i> _w ^c	0.037	0.047
<i>S</i> ^d	1.338	1.538

^a Details in common: *T* = 25 °C, *I* > 3σ(*I*). ^b *R* = Σ(|*F*_o| - |*F*_c|)/Σ|*F*_o|. ^c *R*_w = [Σw(|*F*_o| - |*F*_c||)²/Σw|*F*_o|²]^{1/2}. ^d Goodness of fit = [Σw(|*F*_o| - |*F*_c||)²/(*N*_o - *N*_p)]^{1/2}.

Table 2. Selected Bond Distances (Å) and Bond Angles (deg) for Compound **1**

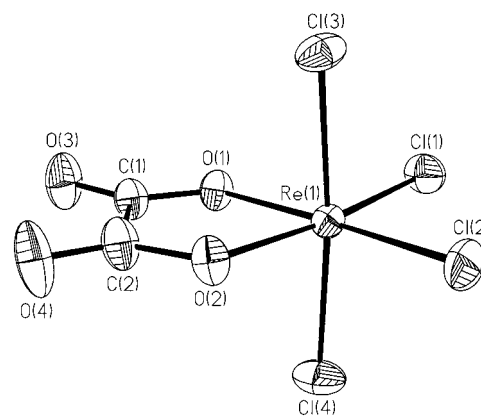
Distances			
Re(1)–O(1)	2.029(4)	Re(1)–O(2)	2.035(5)
Re(1)–Cl(1)	2.341(2)	Re(1)–Cl(2)	2.329(2)
Re(1)–Cl(3)	2.338(2)	Re(1)–Cl(4)	2.350(2)
Angles			
O(1)–Re(1)–O(2)	79.8(2)	O(1)–Re(1)–Cl(2)	173.2(1)
O(1)–Re(1)–Cl(1)	91.0(1)	O(1)–Re(1)–Cl(3)	87.8(1)
O(1)–Re(1)–Cl(4)	88.5(1)	O(2)–Re(1)–Cl(2)	93.6(1)
O(2)–Re(1)–Cl(1)	170.7(1)	O(2)–Re(1)–Cl(3)	88.2(2)
O(2)–Re(1)–Cl(4)	87.0(2)	Cl(2)–Re(1)–Cl(1)	95.7(1)
Cl(2)–Re(1)–Cl(3)	90.7(1)	Cl(2)–Re(1)–Cl(4)	92.5(1)
Cl(1)–Re(1)–Cl(3)	90.4(1)	Cl(1)–Re(1)–Cl(4)	93.8(1)
Cl(3)–Re(1)–Cl(4)	174.4(1)		

positions and refined as riding atoms with a fixed isotropic thermal parameter. Full-matrix least-squares refinements were carried out by minimizing the function Σw(|*F*_o| - |*F*_c||)² with *w* = 1.000/[σ²(*F*_o) + *q*(*F*_o)²], where *q* = 0.0009 (**1**) and 0.0010 (**2**). Models reached convergence with values of the *R* and *R*_w indexes listed in Table 1. The residual maxima and minima in the final Fourier-difference maps were 0.81 and -0.83 e Å⁻³ for **1** and 2.01 and -1.54 e Å⁻³ for **2**. Solutions and refinements were performed with the SHELXTL PLUS system.¹⁴ The final geometrical calculations were carried out with the PARST program.¹⁵ The graphical manipulations were performed using the XP utility of the SHELXTL PLUS system. Main interatomic bond distances and angles are listed in Tables 2 (**1**) and 3 (**2**).

Density Functional Theory (DFT) Calculations. All the calculations were performed with the help of the Gaussian 94 program¹⁶ and using the double-zeta pseudopotential basis set (LanL2DZ).¹⁷ The adiabatic connection method with three parameters (B3LYP)¹⁸ was used, mixing the Hartree–Fock contribution for the exchange with generalized gradient approximation functionals.¹⁹ Atomic spin densities were calculated through the natural bond orbital analysis.²⁰

Table 3. Selected Bond Distances (Å) and Bond Angles (deg) for Compound **2**

Distances			
Re(1)–O(1)	2.054(5)	Re(1)–O(2)	2.039(5)
Re(1)–Cl(1)	2.328(2)	Re(1)–Cl(2)	2.328(2)
Re(1)–Cl(3)	2.338(2)	Re(1)–Cl(4)	2.360(2)
Cu(1)–N(1)	1.995(6)	Cu(1)–N(2)	2.001(6)
Cu(1)–N(3)	1.985(6)	Cu(1)–N(4)	2.005(6)
Angles			
O(1)–Re(1)–O(2)	79.7(2)	O(1)–Re(1)–Cl(2)	171.5(1)
O(1)–Re(1)–Cl(1)	92.8(1)	O(1)–Re(1)–Cl(3)	88.0(1)
O(1)–Re(1)–Cl(4)	86.8(1)	O(2)–Re(1)–Cl(2)	91.9(2)
O(2)–Re(1)–Cl(1)	172.3(2)	O(2)–Re(1)–Cl(3)	88.2(2)
O(2)–Re(1)–Cl(4)	86.2(2)	Cl(2)–Re(1)–Cl(1)	95.7(1)
Cl(2)–Re(1)–Cl(3)	92.2(1)	Cl(2)–Re(1)–Cl(4)	92.2(1)
Cl(1)–Re(1)–Cl(3)	93.1(1)	Cl(1)–Re(1)–Cl(4)	91.9(1)
Cl(3)–Re(1)–Cl(4)	173.0(1)	N(1)–Cu(1)–N(2)	82.1(2)
N(1)–Cu(1)–N(3)	157.5(2)	N(1)–Cu(1)–N(4)	106.3(2)
N(2)–Cu(1)–N(3)	99.7(2)	N(2)–Cu(1)–N(4)	153.3(2)
N(3)–Cu(1)–N(4)	82.3(2)		

**Figure 1.** Perspective drawing of complex **1** showing the atom numbering. Thermal ellipsoids are plotted at 30% probability level.

Results and Discussion

Description of the Structures. Both compounds **1** and **2** contain the [ReCl₄(ox)]²⁻ anionic complex. The charge is counterbalanced by means of [As(C₆H₅)₄]⁺ cations in **1**, whereas [ReCl₄(ox)]²⁻ and [Cu(bipy)]₂²⁺ units are linked through the oxalato group to form the neutral [Cl₄Re(ox)Cu(bipy)]₂ complex in **2**. A perspective drawing of the anion complex in **1** showing the atom numbering is depicted in Figure 1. Neutral units of **2** and the [Cu(bipy)]₂ fragment with the atom numbering are shown in Figure 2a and b, respectively. Each [ReCl₄(ox)] unit contains a Re(IV) atom in a distorted octahedral geometry, being bonded to a didentate oxalato group and four chloride anions. No significant differences were found in the Re–Cl [average value 2.340(2) Å in **1** and 2.339(2) Å in **2**] and Re–O [average value 2.032(5) Å in **1** and 2.047(5) Å in **2**] bond distances. These values are in agreement with those found in the literature.^{9c,12} Bonding angles are close to the ideal values except for O(1)–Re–O(2) [79.8° (**1**) and 79.7° (**2**)] which corresponds to the bite angle of the didentate oxalato ligand. The O(1), O(2), Cl(1), and Cl(2) set of atoms constitute the best equatorial plane around Re, the largest deviation from planarity being 0.004 Å for O(1) (**1**) and 0.017(5) Å for O(2) (**2**). The Re atom is only 0.025(1) (**1**) and 0.019(1) Å (**2**) out of this plane. The carbon–oxygen bond distances are in agreement with those reported for the coordinated oxalato group.²¹ The oxalato ligand is planar

(14) SHELXTL-PLUS, Version 4.11/V; Siemens Analytical X-ray Instruments Inc.: Madison, WI, 1990.

(15) Nardelli, M. *Comput. Chem.* **1983**, *7*, 95.

(16) GAUSSIAN 94; Gaussian Inc.: Pittsburgh, PA, 1994.

(17) (a) Hay, P. J.; Wadt, W. R. *J. Chem. Phys.* **1985**, *82*, 270. (b) Wadt, W. R.; Hay, P. J. *J. Chem. Phys.* **1985**, *82*, 284. (c) Hay, P. J.; Wadt, W. R. *J. Chem. Phys.* **1985**, *82*, 299.

(18) Becke, A. D. *J. Chem. Phys.* **1993**, *98*, 5648.

(19) (a) Becke, A. D. *Phys. Rev. A* **1988**, *38*, 3098. (b) Lee, C.; Yang, W.; Parr, R. G. *Phys. Rev. B* **1988**, *37*, 785.

(20) Weinhold, F.; Carpenter, J. E. In *The Structure of Small Molecules and Ions*; Plenum Press: New York, 1988; p 227.

(21) Oldham, C. In *Comprehensive Coordination Chemistry*; Wilkinson, G.; Gillard, R. D.; McCleverty, J. A., Eds.; Pergamon Press: New York, 1987; Vol. 2, p 444.

in both compounds and it forms a dihedral angle of $4.0(1)^\circ$ (**1**) and $9.8(1)^\circ$ (**2**) with the mean equatorial plane.

$[\text{ReCl}_4(\text{ox})]^{2-}$ anions are packed with bulky tetraphenylarsonium cations in **1**. The complex anions are well separated from each other in the resulting tridimensional ionic lattice. Each one has other twelve neighboring anions at distances varying in the range 10–15 Å, the shortest $\text{Re}\cdots\text{Re}$ distance being 10.345 Å. This large separation precludes any contact between ligand atoms of different anions. The closest atoms, O(4) and Cl(1c) with $(c) = x, -1 + y, z$, are at 5.492(6) Å, and the shortest $\text{Cl}\cdots\text{Cl}$ distance is 7.209 Å. $[\text{As}(\text{C}_6\text{H}_5)_4]^+$ cations show the expected tetrahedral geometry with bond angles around As varying in the range $108.3(3)^\circ$ – $111.3(3)^\circ$.

The Cu(II) ion in compound **2** shows a very distorted five-coordinated geometry, being bonded to four nitrogen atoms from two bipy molecules and an oxygen atom, O(3), from an oxalato group. The oxalate group adopts an unusual bridging mode given that it acts simultaneously as a didentate and monodentate ligand toward rhenium and copper, respectively. The equatorial positions are occupied by the nitrogen atoms whereas the apical one is filled by the oxygen atom. Cu–N distances average 1.996(2) Å, and their values are in the range found for similar compounds.²² The Cu–O distance is very large (2.650(2) Å), and this value remains within the range reported for axial $\text{Cu}^{\text{II}}\text{—O}$ bonds (2.22–2.89 Å).²³ The basal plane geometry is distorted toward the tetrahedron: the dihedral angle between the planes defined by N(3), Cu(1), N(4) and N(1), Cu(1), N(2) is $37.6(2)^\circ$ and the N(1)–Cu(1)–N(3) and N(2)–Cu(1)–N(4) angles are $157.3(2)^\circ$ and $153.3(2)^\circ$, respectively. The pyridyl rings of the bipy ligand are planar as expected, the maximum deviation from the mean planes being 0.029(10) Å at the C(13) atom. The bipy ligand as a whole is quite planar, the dihedral angles between the two pyridyl rings being 5.4° and 6.1° . The values of the angle subtended at the metal atom by the chelating bipy [average $82.2(2)^\circ$] are significantly reduced respect to the ideal value of 90° . The carbon–carbon and carbon–nitrogen bond distances are in agreement with those reported in similar complexes.²²

The $\text{Re}\cdots\text{Cu}$ distance in the $[\text{Cl}_4\text{Re}(\text{ox})\text{Cu}(\text{bipy})_2]$ unit is 4.798(1) Å. These units are arranged in such a way that the Cl(2) chlorine atom of one of them points toward the copper atom of a neighboring one. The resulting Cu–Cl(2) distance, 3.352(2) Å, is over the sum of the van der Waals radii and consequently it is a nonbonding distance. Nevertheless, it could be seen as a very weak bond and the Cu(II) environment may be alternatively described as a distorted octahedron. In this way, the heterobimetallic unit linked together would constitute a chain. In fact, the intermolecular $\text{Re}\cdots\text{Cu}$ distance through the chloro “bridge”, 4.658(1) Å, is somewhat shorter than the intramolecular distance. The copper–chloride bond formation is probably disfavored by the impossibility of the four nitrogen atoms of the two bipy ligands to be coplanar, due to steric effects. The Re–Cu chains have an helicoidal conformation and each one is surrounded by other six. The value of the shortest interchain rhenium–copper separation [8.447(2) Å for $\text{Re}(1)\cdots\text{Cu}(1c)$ and $\text{Re}(1)\cdots\text{Cu}(1d)$ with $(c) = 1 + x, y, z$ and $(d) = -1 + x, y, z$] is much greater than the two intrachain ones. No $\text{Cl}\cdots\text{Cl}$ contacts between different chains are observed, the

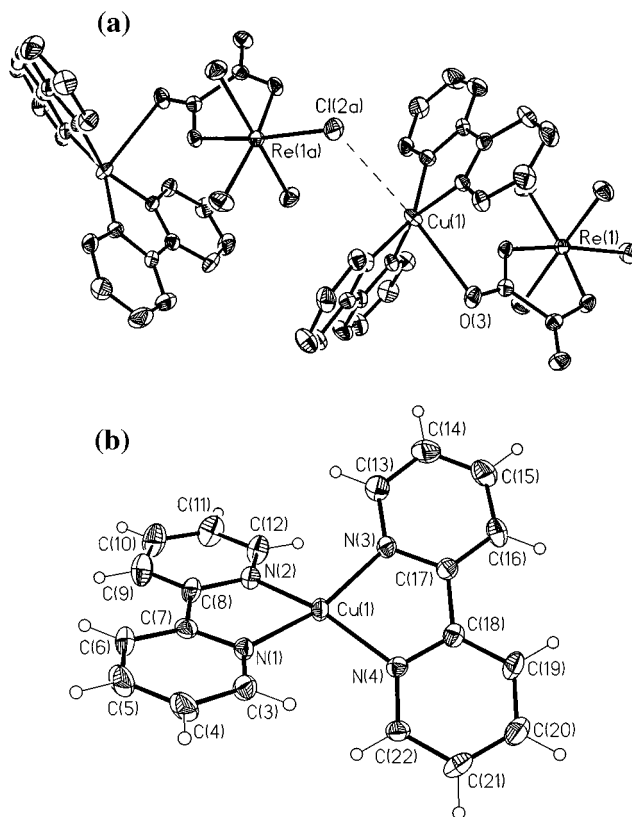


Figure 2. (a) Perspective drawing of two units of complex **2** showing the weak interaction between them through a chloro bridge. (b) Perspective drawing of the $[\text{Cu}(\text{bipy})_2]$ fragment of **2** showing the atom numbering. The $[\text{ReCl}_4(\text{ox})]$ fragment is as in **1**. Thermal ellipsoids are plotted at 30% probability level.

shortest chloro–chloro distance being 5.267 Å for $\text{Cl}(4)\cdots\text{Cl}(4e)$ [$(e) = -x, -y, 1 - z$].

Magnetic Properties. In this section, we will present (i) first the magnetic properties of **1** together with those of selected mononuclear $(\text{cat})_2[\text{ReCl}_6]$ compounds ($\text{cat} = \text{K}^+, \text{NBut}_4^+, \text{AsPh}_4^+$) aiming at understanding the magnetic behavior of this family of compounds. (ii) The conclusions we have obtained will allow us to carry out a thorough analysis of the magnetic properties of the heterobimetallic complex **2** in a second step. (iii) Finally, the analysis of the exchange pathways in **2** will be enlightened through spin density calculations by using the DFT methodology.

(i) The magnetic properties of complexes **1** and $(\text{cat})_2[\text{ReCl}_6]$ under the form of $\chi_{\text{M}}T$ versus T (χ_{M} being the molar magnetic susceptibility) are shown in Figure 3. The inset shows the low-temperature region for **1** and the tetrabutyl- and tetraphenyl-derivatives. In the case of the potassium salt, the $\chi_{\text{M}}T$ value rapidly decreases from room temperature and it vanishes at very low temperatures. The susceptibility curve exhibits a maximum at 12.5 K indicating the presence of antiferromagnetic interactions.²⁴ This cooperative-type transition has been confirmed by heat capacity measurements²⁵ with a maximum at ca. 11.9 K which represents the transition to the antiferromagnetic state and its magnetic ordering has been determined by neutron-diffraction studies.²⁶ This magnetic coupling can be understood taking into account that a greater degree of π -bonding occurs in the third-row transition metal ions, which is accompanied

(22) (a) Harrison, W. D.; Hathaway, B. J. *Acta Crystallogr., Sect. B* **1979**, *35*, 2910. (b) Foley, J.; Tyagi, S.; Hathaway, B. J. *J. Chem. Soc., Dalton Trans.* **1984**, 1.

(23) Hathaway, B. J. In *Comprehensive Coordination Chemistry*; Wilkinson, G., Gillard, R. D., McCleverty, J. A., Eds.; Pergamon Press: New York, 1987; Vol. 5, p 603.

(24) Busey, R. H.; Sonder, E. *Chem. Phys.* **1962**, *36*, 93.

(25) Busey, R. H.; Dearman, H. H.; Gilbert, R. B. *J. Phys. Chem.* **1962**, *66*, 82.

(26) Smith, H. G.; Bacon, G. E. *J. Appl. Phys.* **1966**, *37*, 979.

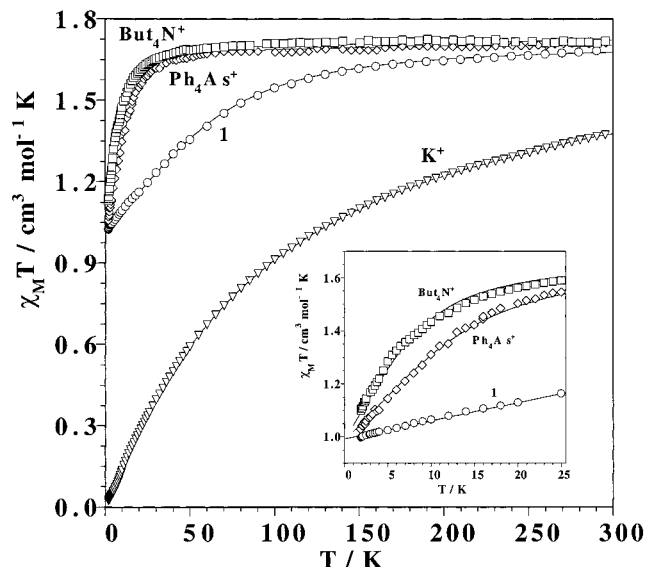
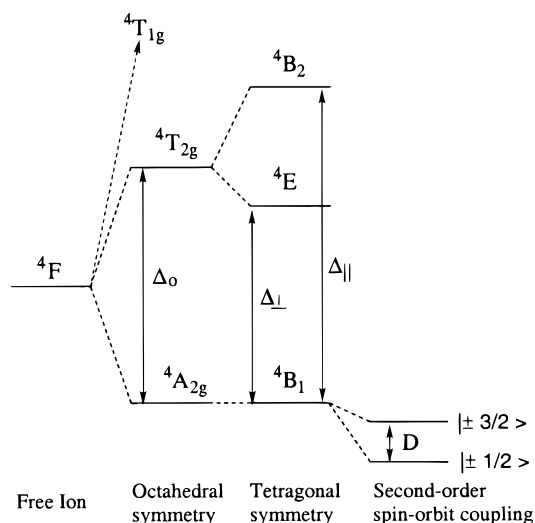


Figure 3. Thermal dependence of $\chi_M T$ for **1**, $K_2[ReCl_6]$, $(NBu_4)_2[ReCl_6]$, and $(AsPh_4)_2[ReCl_6]$. The solid lines are the calculated curves (see text).

by an increased chance of finding the magnetic electron on the ligand atoms. Antiferromagnetic interactions may be transmitted by bonding arrangements such as $M-L \cdots L-M$. This is the case for the potassium salt where the shortest intermolecular chloro-chloro separation is ca. 3.62 Å.²⁷ As the size of the cation increases, the intermolecular chloro-chloro distances also increase and a weaker antiferromagnetic coupling is to be expected. In this regard, bulky cations such as tetrabutylammonium and tetraphenylarsonium should lead to this situation. In fact, the magnetic curves of **1** (the shortest chloro-chloro distance is 7.23 Å) and $(cat)_2[ReCl_6]$ ($cat = NBu_4^+$, $AsPh_4^+$) show that the $\chi_M T$ values remain nearly constant in a wide range of temperatures and smoothly decrease at low temperatures. In principle, the slight decrease of $\chi_M T$ at low temperature in this family could be attributed to intermolecular interactions and/or zero-field splitting (zfs) effects. The presence of a ligand-field component of symmetry lower than cubic can cause the magnetic moment to vary with T , as the spin degeneracy of the $^4A_{2g}$ ground state is then lifted. The fact that the values of $\chi_M T$ tend to a finite value of ca. 1 cm³ mol⁻¹ K (see inset of Figure 3) indicates that, most likely, the zero-field splitting is the responsible factor for the slight decrease of $\chi_M T$. For a d^3 ion in an octahedral environment, the first excited state is $^4T_{2g}$ arising from the 4F free-ion ground state. Under a tetragonal distortion, this state is split into an orbital singlet 4B_2 and an orbital doublet 4E at energies $\Delta_{||}$ and Δ_{\perp} , respectively. This is the case for $[ReCl_6]^{2-}$ in the NBu_4^+ and $AsPh_4^+$ salts. The actual symmetry of $[ReCl_4(ox)]^{2-}$ in **1** is still lower, C_{2v} . For this point group, the orbital doublet 4E is splitted into two orbital singlets 4B_1 and 4B_2 at energies Δ_x and Δ_y , respectively. However, due to the strict equivalence of the x and y axes in the six-coordinated $[ReCl_4(ox)]^{2-}$ entity, both singlets remain degenerated, that is $\Delta_x = \Delta_y = \Delta_{\perp}$. So, Scheme 1 applies for all these monomeric complexes. The quartet spin ground state, $^4A_{2g}$ is removed by the combined action of the spin-orbit interaction and the tetragonal crystal field leading to two Kramers doublets (zero-field splitting). The $^4T_{2g}$ splitting is related to the zero-field splitting of the ground state through eq 1,²⁸ where λ is the spin-orbit coupling parameter and the

Scheme 1



meaning of the remaining terms is clear from Scheme 1.

$$D = 8\lambda^2 \left(\frac{1}{\Delta_{\perp}} - \frac{1}{\Delta_{||}} \right) \quad (1)$$

Formally, this behavior can be treated as an $S = 3/2$ spin state under the action of the spin Hamiltonian $H = D[S_z^2 - 1/3 S(S+1)] + g_{||}\beta H_z S_z + g_{\perp}\beta(H_x S_x + H_y S_y)$ where DS_z^2 represents the splitting into two Kramers doublets in the absence of a magnetic field. In the present notation, positive D values stabilize the $\pm 1/2$ state. The expression of the magnetic susceptibility in eqs 2 and 3 is easily derived from the above-mentioned Hamiltonian,² the parameters therein involved having their usual meaning.

$$\chi_{||} = \frac{N\beta^2}{4kT} g_{Re||}^2 F_{D||} \quad (2)$$

$$\chi_{\perp} = \frac{N\beta^2}{4kT} g_{Re\perp}^2 F_{D\perp} \quad (3)$$

where

$$F_{D||} = \frac{1 + 9 \exp\left(-\frac{D}{kT}\right)}{1 + \exp\left(-\frac{D}{kT}\right)} \quad (4)$$

$$F_{D\perp} = \frac{4 + 6\frac{kT}{D} \left[1 - \exp\left(-\frac{D}{kT}\right) \right]}{1 + \exp\left(-\frac{D}{kT}\right)} \quad (5)$$

Least-squares fitting of the experimental data through this expression leads to $D = 60(5)$ cm⁻¹, $g_{||} = 1.87(1)$, and $g_{\perp} = 1.84(2)$ for **1**, $D = 13(2)$ cm⁻¹ and $g_{||} = g_{\perp} = 1.87(1)$ for the tetraphenylarsonium derivative, and $D = 9(1)$ cm⁻¹ and $g_{||} = g_{\perp} = 1.87(1)$ for the tetrabutylammonium compound. It deserves to be noted that the quality of the fit is very good even at very low temperatures without the inclusion of intermolecular magnetic interactions.

Values of $|D|$ about ca. 10 cm⁻¹ have already been reported for other hexahalorhenate(IV) and hexahaloosmate(V) com-

(27) Grundy, H. D.; Brown, I. D. *Can. J. Chem.* **1970**, *48*, 1151.

(28) Figgis, B. N. *Trans. Faraday Soc.* **1960**, *56*, 1553.

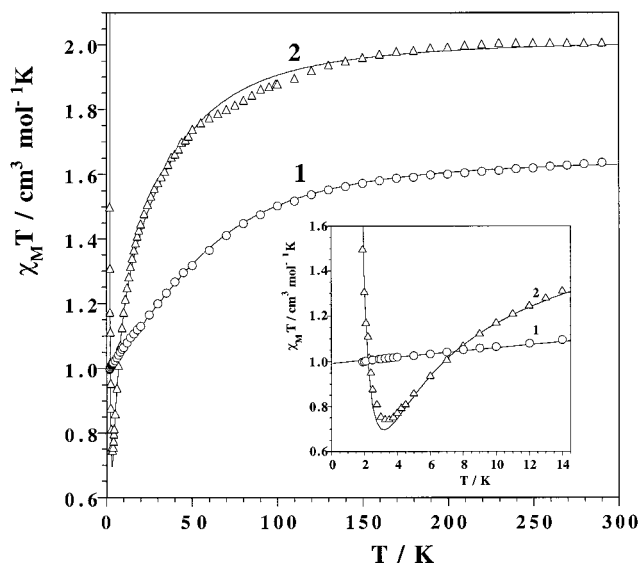


Figure 4. Thermal dependence of $\chi_M T$ for **1** and **2**. The solid lines are the calculated curves (see text).

pounds.^{29,30} These relatively large values of D respect to those expected for isoelectronic first-row transition metal ions can be understood keeping in mind the large value of the spin-orbit parameter of the third row transition elements (λ values of 90 and 1100 cm^{-1} for Cr(III) and Re(IV) single-ions, respectively).⁷ The rhenium atom in complex **1** is coordinated by an oxalate ligand and four chlorine atoms (C_{2v}). A greater crystal field component of symmetry lower than cubic is to be expected because the substantial difference between these two types of ligands and consequently, a larger D value as observed. Given that the ligand field strength for complexes $[\text{ReCl}_6]^{2-}$ is ca. 30 000 cm^{-1} and using a λ value of 750 cm^{-1} (after its reduction by covalency effects, k ca. 0.65),³¹ a ${}^4T_{2g}$ splitting ($\Delta_{||} - \Delta_{\perp}$) of ca. 2000 (for hexahalo complexes) and 12 000 cm^{-1} (for compound **1**) can be easily estimated through eq 1.

The magnetic behavior of this type of magnetically isolated mononuclear rhenium(IV) complexes can be understood from the above theoretical point of view. In fact, at low temperatures where $kT \ll |D|$, the expressions of the magnetic susceptibility (eqs 2 and 3) takes the form of eq 6, where χ_{av} is the average powder magnetic susceptibility and $g = g_{||} = g_{\perp}$. A value of $\chi_{av} T$ ca. 1.0 $\text{cm}^3 \text{mol}^{-1} \text{K}$ can be calculated through eq 6. Consequently, at low temperatures these compounds can be regarded as Ising spin- $1/2$ systems³² with a magnetic moment of 2.8 μ_B ($\chi_{av} T$ ca. 1 $\text{cm}^3 \text{mol}^{-1} \text{K}$).

$$\chi_{av} = \frac{3N\beta^2 g^2}{4kT} \quad (6)$$

(ii) The magnetic properties of **2** under the form of $\chi_M T$ versus T plot (χ_M being the magnetic susceptibility per $\text{Re}^{\text{IV}}\text{Cu}^{\text{II}}$ heterobinuclear unit) is shown in Figure 4. The $\chi_M T$ data of **1** are also included for comparison. $\chi_M T$ for **2** at room temperature is 2.02 $\text{cm}^3 \text{mol}^{-1} \text{K}$, a value which is as expected for an uncoupled $\text{Re}^{\text{IV}}-\text{Cu}^{\text{II}}$ pair. This value decreases upon cooling,

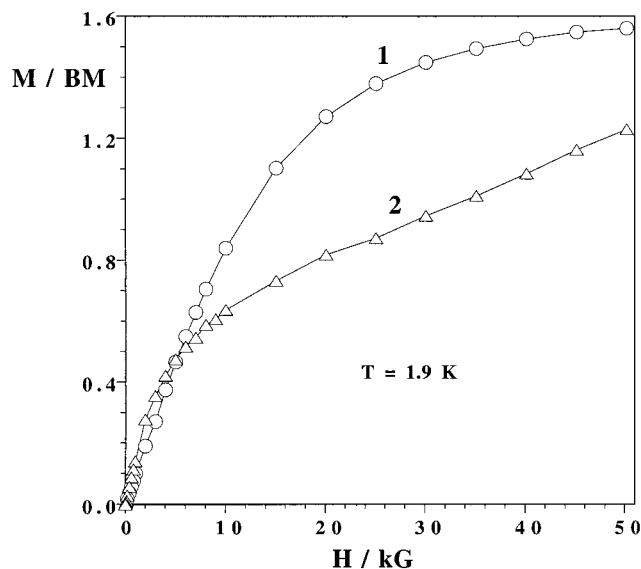


Figure 5. Field dependence of the magnetization for complexes **1** and **2** at 1.9 K.

it reaches minimum at 3.3 K (see inset of Figure 4) and then sharply increases at lower temperatures. It deserves to be noted that the $\chi_M T$ value at the minimum is ca. 0.7 $\text{cm}^3 \text{mol}^{-1} \text{K}$, a value which is even smaller than that of compound **1** at the same temperature. This feature is indicative that antiferromagnetic coupling between Re(IV) and Cu(II) occurs in **2** and it rules out the possibility of ferromagnetic interaction between these metal ions. The field dependence of the magnetization for complexes **1** and **2** at 1.9 K (see Figure 5) clearly support the occurrence of antiferromagnetic interactions in **2**: while the magnetization plot for **1** tends to a saturation value of M ca. 1.6 μ_B per rhenium atom, the corresponding plot for **2** presents an inflection point at ca. 0.85 μ_B per a rhenium-copper pair and its maximum value of M at the highest magnetic field available is still smaller than that for complex **1**.

The presence of a minimum in the $\chi_M T$ curve of **2** suggests that we are faced with a ferrimagnetic chain.² As commented in the structural discussion, compound **2** can be viewed as an alternating bimetallic chain with two weak intrachain magnetic coupling parameters J and j , one through the oxalate-oxygen atom O(3) and the other through the Cl(2) atom.

We now consider the related questions of the choice of the magnetic exchange model and relative size of zero-field splitting and magnetic exchange parameters. From the simplest consideration, we expected that if the exchange is dominant, then Heisenberg-like behavior could be applied. But if the zfs is dominant, an Ising spin- $1/2$ would be preferred. Actually as discussed above, we observe a large D value and in addition the values of the exchange coupling parameters are expected to be weak due to the long distances between the interacting centers through the bridging oxalate-oxygen and single chloro atoms. So, a model of Heisenberg exchange and small D is inappropriate. Although expressions for the magnetic susceptibility of a spin- $1/2$ Ising chain³³ and for the ${}^4A_{2g}$ term with zfs² are each available, the combination of both has not been done to our knowledge. To analyze the magnetic susceptibility data of **2**, we have used the approach which consists of assuming that the susceptibility is given by that of the ${}^4A_{2g}$ term including zfs, modulated by a factor predicted from the Ising model^{30,33}

(29) Reynolds, P. A.; Moubaraki, B.; Murray, K. S.; Cable, J. W.; Engelhardt, L. M.; Figgis, B. N. *J. Chem. Chem. Soc., Dalton Trans.* **1997**, 263.

(30) Reynolds, P. A.; Cristopher, D. D.; Figgis, B. N.; Henderson, M. J.; Moubaraki, B.; Murray, K. S. *J. Chem. Chem. Soc., Dalton Trans.* **1992**, 2309.

(31) Eisenstein, J. C. *J. Chem. Phys.* **1961**, *34*, 1628.

(32) Ising, E. Z. *Phys.* **1925**, *31*, 253.

(33) Coronado, E.; Drillon, M.; Nugteren, P. R.; de Jongh, L. J.; Beltrán, D. *J. Am. Chem. Soc.* **1988**, *110*, 3907.

of the magnetic exchange with the parameters J and j (eqs 7 and 8). This is possible because the susceptibility in the high-temperature region of **2** may be described by two contributions, the susceptibility of the $^4A_{2g}$ term (with zfs) and that one uncoupled copper(II) ion, whereas in the low-temperature region it would be described as a chain of $S_{\text{eff}} = 1/2$ with different local g values³³ (g_{Cu} and g_{Re}). In this approach χ_{\parallel} and χ_{\perp} are defined by eqs 7 and 8, respectively, $F_{\text{D}\parallel}$ and $F_{\text{D}\perp}$ being previously defined in eqs 4 and 5. The relevant spin Hamiltonian is expressed by eq 9.

$$\chi_{\parallel} = \frac{N\beta^2}{4kT}(g_{\text{Cu}\parallel}^2 + g_{\text{Re}\parallel}^2 F_{\text{D}\parallel})F_{\text{J}\parallel} \quad (7)$$

$$\chi_{\perp} = \frac{N\beta^2}{4kT}(g_{\text{Cu}\perp}^2 + g_{\text{Re}\perp}^2 F_{\text{D}\perp})F_{\text{J}\perp} \quad (8)$$

where

$$F_{\text{J}\parallel} = \frac{\exp\left(\frac{J_+}{kT}\right) + R^2 \exp\left(-\frac{J_+}{2kT}\right)}{(1 + R^2)\cosh\left(\frac{J_-}{2kT}\right)}$$

$$F_{\text{J}\perp} = \frac{2kT}{j} \tan gh\left(\frac{j}{4kT}\right) + \frac{1}{2} \sec h^2\left(\frac{j}{4kT}\right)$$

$$J_{\pm} = \frac{J \pm j}{2}, g_{\pm} = \frac{g_{\text{Re}} \pm g_{\text{Cu}}}{2}, R = \frac{g_-}{g_+}$$

$$H = \sum_i \{ -JS_{2i-1}^z S_{2i}^z - jS_{2i}^z S_{2i+1}^z + g_{\parallel\text{Cu}}\beta S_{2i-1}^z H_z + g_{\parallel\text{Re}}\beta S_{2i}^z H_z + g_{\perp\text{Cu}}\beta(S_{2i-1}^x H_x + S_{2i-1}^y H_y) + g_{\perp\text{Re}}\beta(S_{2i}^x H_x + S_{2i}^y H_y) + D[(S_{2i}^z)^2 - 5/4] \} \quad (9)$$

This approach allows us to reproduce theoretically (solid line in Figure 4) the experimental susceptibility data of **2** in the whole temperature range, the parameters being $J = -25(1) \text{ cm}^{-1}$, $j = -13.0(5) \text{ cm}^{-1}$, $g_{\parallel\text{Re}} = 1.86(2)$, $g_{\perp\text{Re}} = 1.82(3)$, $g_{\parallel\text{Cu}} = 2.33(3)$, $g_{\perp\text{Cu}} = 2.01(1)$, and $D = 53(5) \text{ cm}^{-1}$. Note that the values of J and j that we have obtained through this approach are referred to an $S_{\text{eff}} = 1/2$ and aiming at comparing them with the D value (which is referred to a real $S = 3/2$), they should be reduced by a factor about three ($J/3 = -8.3 \text{ cm}^{-1}$ and $j/3 = -4.3 \text{ cm}^{-1}$). The value of D that we have obtained by fit is very close to that observed for complex **1** and it is much greater than those of J and j as required by the model. We conclude that Re(IV) in **2** exhibits a large zfs together with weak antiferromagnetic interactions with Cu(II) in such a way that **2** can be well described as a ferrimagnetic chain by using an Ising spin- $1/2$ model with alternating g factors. The magnetic interactions are sufficiently large that deficiencies in this simple approach may well produce systematic errors in the calculated parameters, but the overall description is out of question.

(iii) At first sight, the efficiency of the intrachain exchange pathways in complex **2** to mediate magnetic interactions is quite surprising. Looking at the copper(II) ion, its unpaired electron is mainly delocalized in the four Cu–N equatorial bonds and because of its flattened tetrahedral distortion some spin density is expected to occur in the axial oxalate-oxygen and chloro atoms. However, the great lengths of the copper to axial atom bonds would suggest a negligible magnetic interaction through this pathway. This prediction is reinforced by the fact that the three unpaired electrons of rhenium(IV) are described by π -type

Table 4. Calculated Atomic Spin Densities for $[\text{MCl}_4(\text{ox})]^{z-}$ ($\text{M} = \text{Cr}^{\text{III}}, \text{Re}^{\text{IV}}$)

atom	$[\text{CrCl}_4(\text{ox})]^{3- a}$	$[\text{ReCl}_4(\text{ox})]^{2- a}$	$[\text{ReCl}_4(\text{ox})]^{2- b}$	$[\text{ReCl}_4(\text{ox})]^{2- c}$
Cl(1)	-0.0081	+0.1131	+0.1454	+0.1496
Cl(2)	-0.0081	+0.1131	+0.1454	+0.1477
Cl(3)	-0.0302	+0.0805	+0.1208	+0.1269
Cl(4)	-0.0302	+0.0805	+0.1208	+0.1087
O(1)	-0.0125	+0.0592	+0.0579	+0.0535
O(2)	-0.0125	+0.0592	+0.0579	+0.0597
O(3)	+0.0093	+0.0374	+0.0296	+0.0271
O(4)	+0.0093	+0.0374	+0.0296	+0.0276
C(1)	+0.0064	+0.0070	+0.0076	+0.0008
C(2)	+0.0064	+0.0070	+0.0076	+0.0008
M	+3.0703	+2.4006	+2.2777	+2.2840

^a Optimized geometry structure. ^b After the monomer structure in **1**. ^c After the monomer structure in **2**.

orbitals which have a lower efficiency in mediating exchange coupling than σ orbitals. However, a larger magnetic coupling would be predicted in **2** with respect to what one could expect for compounds containing only first-row transition metal ions because of the great diffuse character of the 5d type orbitals of the rhenium atom as well as its high oxidation state, factors both which lead to significantly greater electronic delocalization. Aiming at understanding the significant intrachain exchange couplings in complex **2**, we performed DFT calculations on the mononuclear $[\text{ReCl}_4(\text{ox})]$ units occurring in **1** and **2**. The computed spin densities are given in the two last columns of Table 4. We computed also the spin densities in the hypothetical Cr(III) complex $[\text{CrCl}_4(\text{ox})]^{3-}$. As its structure is unknown, we used a model whose structure was optimized and for the sake of a direct comparison, an optimized structure of the parent Re(IV) complex was also considered (two first columns in Table 4). This will allow us to compare and analyze the influence of 5d (Re) with respect to 3d (Cr) orbitals as far the spin distribution on the intervening atoms. The atom numbering of the real structures **1** and **2** has been kept in this series.

Prior to discussing the results of these calculations, we recall that two mechanisms, namely (a) the *spin delocalization* and (b) the *spin polarization*, allow for an unpaired electron of a transition metal ion to place some spin density on other atoms of the complex.³⁴ First, an unpaired electron can be described by a molecular orbital Ψ (magnetic orbital) which is expressed as a linear combination of atomic orbitals ϕ_i ($\Psi = \sum_i c_i \phi_i$). The probability of finding the unpaired electron at a particular ϕ_i is related to the square of the coefficient c_i with which that atomic orbital contributes to Ψ . Adopting the convention that the unpaired electron has a positive spin, its delocalization results in a distribution of positive spin density throughout the complex which is determined by the composition of Ψ . The resulting distribution of the spin density is said to arise from a *spin delocalization mechanism*. The corresponding spin density on a given atom is obtained by summing up the spin densities of its atomic orbitals.

Second, the positive spin density on the paramagnetic center may induce some spin density of opposite sign in the atoms bonded to it. This effect propagates through the molecule away from the paramagnetic center, thus generating spin densities of alternating sign. This is referred as a *spin polarization mechanism*. The key point here, is that the net spin density on a particular atomic orbital or atom therefore results from the

(34) Cano, J.; Ruiz, E.; Alvarez, S.; Verdager, M. *Comments Inorg. Chem.* **1998**, *20*, 27.

combination of these two mechanisms. They can add up to give a positive value (when both mechanisms afford a positive spin density) or cancel in part to give either a positive (delocalization mechanism is predominant) or negative (spin polarization is dominant) total spin density.

An inspection of Table 4 reveals that all the spin densities are positive in the case of the Re(IV) complexes, whereas there are positive and negative values in the case of the Cr(III). Moreover, the value of the spin density is greater than three on the chromium atom but significantly smaller than three on the rhenium atom. These results show that the spin delocalization mechanism is dominant in the case of the Re(IV), whereas spin polarization is more important in the case of Cr(III). The large spin delocalization in the Re(IV) complex is responsible for the great spin density on the ligand atoms. However, all the values of spin density on the ligand atoms in the Cr(III) complex, either positive or negative, are very small. In this respect, it is very interesting to compare the spin density values on the Cl(2) and O(3) atoms which would be involved in the bridging pathway as in complex **2**. They are significantly larger in the Re(IV) complexes.

As proposed by McConnell,³⁵ the Hamiltonian describing the magnetic interactions between two paramagnetic centers (in the present case Cu(II) and Re(IV) with local spins of $1/2$ and $3/2$, respectively) is given by eq 10 where J_{ij} accounts for the magnetic interaction between two nearest-neighbors spin densities ρ_i and ρ_j of the bridging atoms. The J and j values from the Hamiltonian given in eq 9 would correspond to eq 11 in the McConnell formalism. It is clear that the larger the spin densities at the bridging atoms are, the greater the exchange coupling is. In fact, a linear correlation between the atomic spin density and the exchange coupling has been observed for oxalato-bridged dinuclear copper(II) complexes recently.³⁴

$$H = -S_{\text{Re}}S_{\text{Cu}} \sum_{i=1}^{n-1} \sum_{j=i+1}^n J_{ij} \rho_i \rho_j \quad (10)$$

$$J_{\text{ReCu}} = \sum_{i=1}^{n-1} \sum_{j=i+1}^n J_{ij} \rho_i \rho_j \quad (11)$$

We would like to finish the present contribution noting that there are two intrachain bridging pathways in **2**, one being twice greater than the other one ($J \approx -25 \text{ cm}^{-1}$ and $j \approx -13 \text{ cm}^{-1}$) and it is not easy to assign them. The copper to oxalato-oxygen O(3) distance is shorter than the copper to chloro atom Cl(2) but the atomic spin density is much more important for the chloro atom. Hoping to give a clear-cut answer to this situation, we have undertaken ab initio calculations on the $\text{Re}^{\text{IV}}\text{-Cu}^{\text{II}}$ model systems.

Acknowledgment. Financial support from the Spanish DGICYT through Project PB97-1397, the Training and Mobility Research Programme from the European Union TMR Contract ERBFMRXCT-980181, and the Italian Ministero dell' Università e della Ricerca Scientifica e Tecnologica is gratefully acknowledged. R.C. and R.G. are indebted to the European Union for a grant (ALFA Programme ALR/B7-3011/94.04-5.0273(9)).

Supporting Information Available: Tables of crystal data and structure refinement, anisotropic displacement coefficients, atomic coordinates and equivalent isotropic displacement parameters for non-hydrogen atoms, H-atom coordinates and isotropic displacement parameters, bond lengths and interbond angles, and least-squares planes. This material is available free of charge via the Internet at <http://pubs.acs.org>.

(35) McConnell, H. M. *J. Chem. Phys.* **1963**, *39*, 1910.